# Mathematical modeling of Stokes flow in petal shaped pipes ⓕ

Zhimin Xu (徐志敏), Siyuan Song (宋思远), Fengxian Xin (辛锋先) ⒾⒹ, and Tian Jian Lu (卢天健)

**COLLECTIONS**

ⓕ This paper was selected as Featured

View Online          Export Citation          CrossMark

## ARTICLES YOU MAY BE INTERESTED IN

Smoothed particle hydrodynamics (SPH) for complex fluid flows: Recent developments in methodology and applications
Physics of Fluids **31**, 011301 (2019); https://doi.org/10.1063/1.5068697

Aerodynamic forces on projectiles used in various sports
Physics of Fluids **31**, 015106 (2019); https://doi.org/10.1063/1.5064700

Capillary surface wave formation and mixing of miscible liquids during droplet impact onto a liquid film
Physics of Fluids **31**, 012107 (2019); https://doi.org/10.1063/1.5064640

AIP Publishing

# Mathematical modeling of Stokes flow in petal shaped pipes (F)

View Online     Export Citation     CrossMark

**Zhimin Xu (徐志敏)**,[1,2,3] **Siyuan Song (宋思远)**,[1,3] **Fengxian Xin (辛锋先)**,[1,3,a]  and **Tian Jian Lu (卢天健)**[1,2,a]

## AFFILIATIONS

[1] State Key Laboratory for Strength and Vibration of Mechanical Structures, Xi'an Jiaotong University, Xi'an 710049,
 People's Republic of China
[2] State Key Laboratory of Mechanics and Control of Mechanical Structures, Nanjing University of Aeronautics and Astronautics,
 Nanjing 210016, People's Republic of China
[3] MOE Key Laboratory for Multifunctional Materials and Structures, Xi'an Jiaotong University, Xi'an 710049,
 People's Republic of China

[a] fengxian.xin@gmail.com and tjlu@nuaa.edu.cn

## ABSTRACT

A theoretical model is developed to characterize fully developed laminar flow (Stokes flow) in idealized petal shaped pipes by regarding the pipe wall as a circular boundary having sinusoidal perturbation (or, equivalently, surface roughness). Built upon the method of perturbation, the model quantifies the effects of the relative roughness and wave number of the pipe boundary on the Stokes flow. Approximate solutions of the velocity field, pressure gradient, and static flow resistivity are obtained. The same approach together with the method of Fourier transform is used to deal with low Reynolds flow in pipes having other cross-sectional morphologies such as triangle and square. Results obtained from computational fluid dynamics simulations are used to validate the theoretical model predictions, with good agreement achieved. The presence of surface roughness causes periodic fluctuation and global offset of velocity distribution and enlarges both the pressure gradient and static flow resistivity in petal shaped pipes.

## I. INTRODUCTION

How surface roughness affects fluid flow is a fundamental problem in fluid mechanics.[1,2] Von Mises[3] first introduced the concept of relative roughness to characterize the influence of surface roughness. Colebrook et al.[4,5] and Nikuradse[6] carried out detailed experimental and theoretical studies on the effect of the relative roughness and Reynolds number, providing a classic way to analyze the problem. They found that this effect can be divided into three regions, the laminar region, the transition region, and the turbulence zone; in the laminar region, the influence of the rough boundary can be ignored. A series of empirical formulas were also developed to describe the relationships between relevant parameters. Based on experimental and theoretical results, Moody[7] plotted the relation diagram between the relative roughness, Reynolds number, and Darcy friction coefficient, which is called the Moody diagram and widely used in industry.

However, these results are not applicable to cases involving large relative roughness for existing studies concerned mainly small values (<5%) of relative roughness. Besides, in existing studies, the specific morphology of surface roughness was not fully discussed.

For simplicity in theoretical and numerical modeling, the rough surface has been commonly assumed to exhibit a periodic structure.[8–12] Kandlikar et al.[13] pointed out that fluid concentration caused by the rough structure is not negligible when the relative roughness becomes relatively large: even in the laminar region, the change in the friction coefficient due to the change in the hydraulic radius affects the fluid field.

Topologically speaking, roughness on the inner surface of a circular pipe may be divided into two main categories. In the first category, the roughness is distributed along the axial direction (i.e., direction of fluid flow) of the pipe, which has been discussed in many studies.[13–15] In the other, the

rough structure is distributed along the circumference of the pipe, implying that its cross-sectional morphology is no longer circular. The present study focuses upon the latter one for it is poorly investigated in the open literature. Specifically, low Reynolds number flows in pipes with petal shaped cross sections are investigated.

The flow in pipe also does much meaning for investigating the acoustic properties of porous medium as it consists of many microtunnels (pores). However, in most practical cases, the pore morphology in the porous medium is not smooth. To address the issue, the acoustical properties of model porous media with simple pore shapes (e.g., square and triangular) have been theoretically studied.[16] In order to quantify the influence of the cross-sectional shape of the pore (e.g., deviation from circular) on complex density and compressibility–two important parameters governing the acoustic properties of the porous medium–the concept of shape factor was introduced.[17] When investigating the sound absorbing ability, as noted by Attenborough,[18] the pore shape with a larger shape factor provides a greater resistance for sound to pass, thus a larger air flow resistivity. In other words, the shape factors for different pore shapes reflect the relative flow resistivities for fluid to pass through these pores. Although the introduction of shape factor makes it easy to understand flow inside pores, there are some limitations to this approach. In addition to frequency correlation, every time a new pore shape is of concern, a series of complex operations need to be carried out to obtain its shape factor. By contrast, the method of perturbation starts with a simplified form of the original problem, which is simple enough to be solved exactly. The method is more like a mathematical technique for finding an approximate solution to a problem, by starting from the exact solution of a related, simpler problem. A critical feature of the technique is a middle step that breaks the problem into "solvable" and "perturbation" parts.[19] In fact, as one of the new methods for analyzing turbulent boundary layers, it has been demonstrated that the perturbation method provides more accurate, yet practical, means for estimating the skin-friction, heat transfer, and separation on aircraft components under flight conditions.[20,21]

In the current study, the modified perturbation method is employed to investigate analytically the fully developed laminar flow at small Reynolds numbers (Stokes flow) inside idealized petal shaped pipes. The pipe wall is taken as a circular boundary having sinusoidal perturbation (or, equivalently, surface roughness). Approximate solutions for velocity distribution, pressure gradient, and static flow resistivity of the petal shaped pipes are obtained. Numerical simulations with computational fluid dynamics (CFD) are performed to validate the analytical model predictions. The influence of key geometrical parameters characterizing the petal shaped cross section on pipe flow is quantified. Furthermore, the same approach together with the method of Fourier transform is used to deal with low Reynolds flow in pipes having other cross-sectional morphologies such as triangle and square.

## II. ANALYSIS OF STOKES FLOW IN PETAL SHAPED PIPES

Figure 1 depicts schematically a wide range of pipes having idealized petal shaped cross sections. For convenience, relative to the case of a smooth circular pipe, the petal-shaped pipe may be taken as a roughened pipe in a way similar to our previous study on surface roughness effects on stokes flow in circular pipes.[22] Let $n$ be the number of waves in the cross-sectional plane of the petal shaped pipe, which represents the density of the periodic rough structure on the pipe wall. According to the definition of relative roughness, $\varepsilon = e/D$ is introduced to quantify the relative altitude of the rough structure, where $D$ is the nominal diameter of the pipe (Fig. 1) and $2e$ is the radical distance between the peak and the valley of the rough structure. Such periodic microstructures are evenly distributed over the circumference of the pipe so that its boundary may be described by

$$\bar{r} = \Gamma(\theta)D, \quad \text{with } \Gamma(\theta) = 0.5 - \varepsilon \sin(n\theta). \tag{1}$$

Here, the cylindrical coordinate system has its origin at the center of the pipe, the $z$-axis is along its axial direction of the
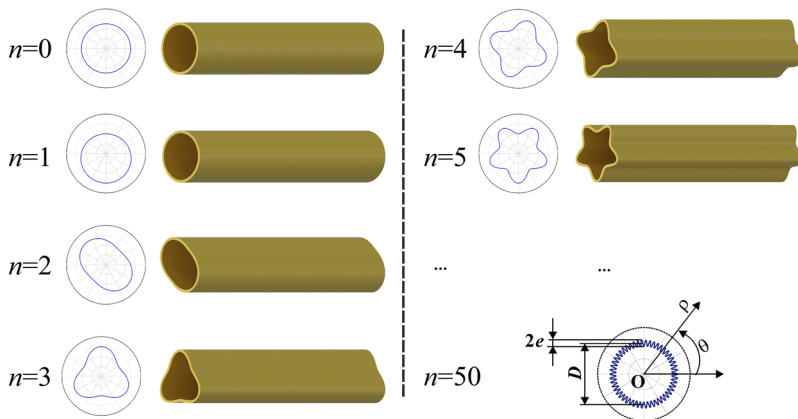


**FIG. 1**. Sketch of petal shaped cross-sectional pipes with different wave numbers.

pipe, and $\rho$, $\theta$ are in the cross-sectional plane, as shown in Fig. 1. A dimensionless coordinate system is defined by setting $r = \rho/D$. So, the geometric boundary line can be expressed as $r = \bar{r}/D = \Gamma(\theta)$.

Mathematically speaking, the dimensionless geometric boundary $\Gamma(\theta)$ of (1) can be treated as a sine-type turbulence on a circle with a radius of 0.5. Having such a complex boundary makes it too difficult to solve directly the flow in the pipe. However, the perturbation method, which replaces the disturbance of the geometric boundary with a disturbance of the fluid field, can provide approximate solutions to the problem in a sophisticated way, as demonstrated below.

## A. Modified perturbation method

With reference to Fig. 1, the case considered is pressure-driven, steady-state flow (i.e., Poiseuille flow) in straight channels with different petal shaped cross sections. Here, the nonlinear Navier-Stokes equation governing the flow of Newtonian incompressible fluid at small Reynolds numbers can be simplified to the linear Stokes equation. As both the characteristic length and characteristic velocity in the problem of Fig. 1 are taken as considerably small, neglecting the inertial term is considered acceptable.[23,24] Due to the linearity of the Stokes equation, it is reasonable to adopt a relatively large range of relative roughness (e.g., [0, 0.1]) for the roughened pipe without a significant loss in accuracy.

For fully developed steady incompressible flow, the dimensionless Stokes equation is

$$0 = -\frac{\partial p}{\partial z} + \left(\frac{1}{r}\frac{\partial}{\partial r}\left(r\frac{\partial}{\partial r}\right) + \frac{1}{r^2}\frac{\partial^2}{\partial \theta^2}\right)u, \qquad (2)$$

where $p$ and $u$ are the pressure and velocity of the fluid. The inner boundary of the petal shaped pipe is assumed to be no-slip, and at the center of the pipe, the flow field is symmetrical. The boundary conditions can thus be written as

$$\begin{aligned} u = 0 \quad &\text{at} \quad r = 0.5 - \varepsilon \sin(n\theta) \\ \frac{\partial u}{\partial r} = 0 \quad &\text{at} \quad r = 0 \end{aligned}. \qquad (3)$$

Assuming that the relative roughness ($\varepsilon$) of the pipe is sufficiently small, one can take the Taylor expansion of the velocity $u(r, \theta)$ about $\varepsilon$ and retain only its zero- and first-order terms as

$$u(r, \theta) = u_0(r, \theta) + \varepsilon u_1(r, \theta) + O(\varepsilon^2), \qquad (4)$$

where $O(\varepsilon^n)$ is defined as the infinitesimal of the $n$-th order. According to the perturbation method, fluid velocity at the boundary can be expressed as

$$u(r, \theta)|_{r=\Gamma(\theta)} = u(r, \theta)|_{r=0.5} - \varepsilon\sin(n\theta)\left(\frac{\partial u(r, \theta)}{\partial r}\right)\Big|_{r=0.5} + O(\varepsilon^2). \qquad (5)$$

In Eq. (5), values at the complex boundary $\Gamma(r, \theta)$ can be obtained through the properties at the simplified boundary $r = 0.5$. As a result, the influence of wall roughness can be reflected by the first-order perturbation term

$\varepsilon\sin(n\theta)\left(\frac{\partial u(r,\theta)}{\partial r}\right)\Big|_{r=0.5}$. Consequently, the following analysis and results are all obtained in the equivalent domain: $r \in (0, 0.5)$, $\theta \in (0, 2\pi)$.

The solution obtained with the zero-order term of the perturbed equation is

$$u_0 = 2 - 8r^2. \qquad (6)$$

This is actually the classical velocity field of Poiseuille flow inside a smooth circular pipe.

The first-order term of the perturbed equation together with the revised boundary condition is given by

$$\begin{aligned} 0 = -\frac{\partial p_1}{\partial z} &+ \left(\frac{1}{r}\frac{\partial}{\partial r}\left(r\frac{\partial}{\partial r}\right) + \frac{1}{r^2}\frac{\partial^2}{\partial \theta^2}\right)u_1 \\ u_1 = -4\sin(n\theta) &+ Q, \quad \text{at} \quad r = \frac{1}{2} \\ \frac{\partial u}{\partial r} = 0 \quad &\quad\quad\quad \text{at} \quad r = 0 \end{aligned}, \qquad (7)$$

where Q is a first-order infinitesimal, i.e., $Q = O(\varepsilon)$. If the boundary condition is not revised by introducing Q, a non-ignorable error will occur. In other words, to be consistent with the physical fact that the cross section of the roughened pipe is closely related to flow resistance, the perturbation of the pipe boundary inevitably affects the pressure drop along the z-axis of the pipe. In fact, the nonlinearity of the boundary curve, serving as the disturbance source, magnifies the high-order terms in the system so that the Q term in Eq. (7) cannot be neglected.

In order to separate the two variables $r$ and $\theta$, taking Fourier transform of the first-order term of velocity $u_1$ in the $\theta$ (circumferential) direction, we find that only three terms remain, namely,

$$u_1 = \varphi_{-1}(r)e^{-(n\theta-\pi/2)i} + \varphi_0(r) + \varphi_1(r)e^{(n\theta-\pi/2)i}, \qquad (8)$$

where $n\theta - \pi/2$ is adopted to make the real part agree with the boundary condition. In fact, $\varphi_{-1}(r)$ and $\varphi_1(r)$ terms represent the periodic fluctuation of flow velocity along the circumferential direction, which is not directly related to the growth of the pressure gradient, while $\varphi_0(r)$ represents the overall offset of velocity along the radial direction. According to Eq. (2), the $\varphi_0(r)$ term is actually responsible for the increased pressure drop due to surface roughness. Substituting Eq. (8) into the governing equations, we arrive at two independent equations for $\varphi_1$ and $\varphi_0$ as

$$\begin{aligned} 0 = r^2\frac{\partial^2 \varphi_1(r)}{\partial r^2} &+ r\frac{\partial \varphi_1(r)}{\partial r} - n^2\varphi_1(r) \\ \varphi_1 = -2, \quad &\text{at} \quad r = 0.5 \\ \frac{\partial \varphi_1}{\partial r} = 0, \quad &\text{at} \quad r = 0 \end{aligned}, \qquad (9)$$

$$\begin{aligned} \frac{\partial p_1}{\partial z} &= \frac{\partial^2 \varphi_0}{\partial r^2} + \frac{1}{r}\frac{\partial \varphi_0}{\partial r} \\ \varphi_0 &= Q, \quad \text{at} \quad r = 0.5. \\ \frac{\partial \varphi_0}{\partial r} &= 0, \quad \text{at} \quad r = 0 \end{aligned} \qquad (10)$$

Due to symmetry, $\varphi_1$ and $\varphi_{-1}$ are complex conjugates. The solution of (9) is given by

$$\varphi_1(r) = -2^{n+1}r^n. \tag{11}$$

As discussed above, this solution does not cause any increase in the pressure gradient.

To get a better understanding of the influence of the petal shaped cross section on the pressure drop, the $\varphi_0$ term is determined next. Solution to (10) can be expressed as

$$\varphi_0(r) = E + Fr^2, \tag{12}$$

where $E(\varepsilon, n)$ and $F(\varepsilon, n)$ are two functions directly related to Q. Since incompressible fluid is assumed, the velocity flux increment in the whole domain should be zero: that is, the conservation of velocity holds,

$$\int_0^{2\pi} \left[ \int_0^{1/2} u_1 r dr \right] d\theta = 0. \tag{13}$$

It has been established that the terms involving $\varphi_1$, $\varphi_{-1}$ have no contribution to the final result because of the integration property of the trigonometric function. Inserting (12) into (13) yields

$$F = -8E. \tag{14}$$

Equation (14) is an approximate expression, helpful for estimating the values of F and E. The precise expressions of $F(\varepsilon, n)$ and $E(\varepsilon, n)$ are determined in Sec. II B.

## B. Solution

Given that the petal shaped cross section blocks fluid flow relative to its smooth counterpart, the blocking effect may be quantified based on the flow fields in two extreme cases. One such limit is when the wave number is so large that the rough structure is extremely dense, i.e., $n \to \infty$. The other limit corresponds simply to the case of smooth pipe, i.e., $n = 0$. One may consider these two extreme cases as asymptotic limits, which means that the pressure drops of the two cases represent the upper and lower bounds, respectively. As the wave number $n$ increases, it becomes more difficult for the fluid to flow through the rough pipe. Correspondingly, the pressure drop increases continuously, approaching the upper limit asymptotically as $n \to \infty$. To describe the two asymptotic limits, for the problem considered in the current study, the logistic function[25] may be adopted. The logistic function is used to approximate the dependence of E and F on $n$ as

$$E = \left( A \frac{2e^{-\frac{1}{12.5}n}}{1 + e^{-\frac{1}{12.5}n}} + B \right), \tag{15}$$

$$F = \left( C \frac{2e^{-\frac{1}{12.5}n}}{1 + e^{-\frac{1}{12.5}n}} + D \right), \tag{16}$$

where A, B, C, and D are four coefficients that are dependent on relative roughness.

When $n \to \infty$, the rough pipe is analogous to a smooth tube with diameter $(1 - 2\varepsilon)D$. Correspondingly, the Poiseuille flow has velocity

$$u_{n=\infty} = 8(1 - 2\varepsilon)^{-4} \left[ (0.5 - \varepsilon)^2 - r^2 \right], \tag{17}$$

which yields

$$\begin{aligned} B &= \left[ 2(1 - 2\varepsilon)^{-2} - 2 \right] / \varepsilon \\ D &= \left[ -8(1 - 2\varepsilon)^{-4} + 8 \right] / \varepsilon \end{aligned} . \tag{18}$$

When $n \to 0$, the rough pipe is analogous to a smooth tube with diameter D. The velocity is

$$u_{n=0} = 2 - 8r^2, \tag{19}$$

from which

$$\begin{aligned} A &= \left[ 2 - 2(1 - 2\varepsilon)^{-2} \right] / \varepsilon \\ C &= \left[ 8(1 - 2\varepsilon)^{-4} - 8 \right] / \varepsilon \end{aligned} . \tag{20}$$

Thus, upon considering the asymptotic limits, the four coefficients A, B, C, and D are determined. Substituting them into Eq. (8), we obtain the velocity field as

$$\begin{aligned} u = & \left[ 2 - 2(1 - 2\varepsilon)^{-2} + \left( 8(1 - 2\varepsilon)^{-4} - 8 \right) r^2 \right] \left( \frac{2e^{-\frac{1}{12.5}n}}{1 + e^{-\frac{1}{12.5}n}} - 1 \right) \\ & - \varepsilon 2^{n+2} r^n \sin(n\theta) + 2 - 8r^2. \end{aligned} \tag{21}$$

The Stokes equation in the $z$-direction is written as

$$\frac{\partial p}{\partial z} = \left( \frac{1}{r} \frac{\partial}{\partial r} \left( r \frac{\partial}{\partial r} \right) + \frac{1}{r^2} \frac{\partial^2}{\partial \theta^2} \right) u. \tag{22}$$

Making use of (21), we calculate the ratio of the average pressure drop (i.e., area-weighted average of $\partial p / \partial z$) across a petal shaped pipe to that across a smooth pipe, resulting in

$$k_f(\varepsilon, n) = \frac{(\partial p / \partial z)_{rough}}{(\partial p / \partial z)_{smooth}} = \frac{1}{(1 - 2\varepsilon)^4} + \left( 1 - \frac{1}{(1 - 2\varepsilon)^4} \right) \frac{2e^{-\frac{1}{12.5}n}}{1 + e^{-\frac{1}{12.5}n}}. \tag{23}$$

To quantify the influence of surface roughness on fluid flow, the concept of static flow resistivity is employed, which is a fluidic parameter reflecting the viscous resistance of the pipe. By definition, the static flow resistivity is the quotient of the air pressure difference across a pipe divided by the volume velocity of airflow through it.[26] So, the static flow resistivity can be expressed as $\sigma = -\Delta P / LU$, with $\Delta P$ being the fluid pressure drop across the pipe, L being the length of the pipe, and U being the average volume velocity of fluid in the pipe. The relative static flow resistivity of the present petal shaped tube is hence

$$\frac{\sigma_{rough}}{\sigma_{smooth}} = \frac{(\Delta P / LU)_{rough}}{(\Delta P / LU)_{smooth}} = k_f, \tag{24}$$

where $\sigma_{smooth} = 8\mu / R^2$ is the static flow resistivity of a smooth tube with radius R. When $\varepsilon = 0$, the relative static flow resistivity is equal to 1. When the wave number $n \to 0$, the relative static flow resistivity takes the minimum 1; when $n \to \infty$, it takes the maximum $1/(1 - 2\varepsilon)^4$. That is, when $n$ is increased, the relative static flow resistivity increases from 1 to $1/(1 - 2\varepsilon)^4$.

## C. Triangular and square cross-sectional pipes

In addition to sinusoidal (petal shaped) cross sections considered above, several common cross-sectional morphologies, such as triangle and square, can be modeled by decomposing their boundary curve functions into series of sinusoidal functions via Fourier transform. This is demonstrated next.

To select a moderate length to apply the proposed modeling approach, the length corresponding to the unit circle is adopted. Thus, the areas of triangle and square are set equal to that of the unit circle, as shown in Fig. 2. According to Eq. (7), the effect of the cross-sectional shape on flow is characterized using the revised boundary condition. For any given shape of the boundary curve, Fourier transform can be expressed by the general form as

$$r_{shape}(\theta) - 0.5 = -\sum_{n=1}^{\infty} \text{sgn}_n \cdot \varepsilon_n \sin(n\theta), \qquad (25)$$

where $\text{sgn}_n$ represents the sign of the $n$-th component. As the model present above, $\varepsilon_n$ is the relative roughness, whose value is positive. To assure the completeness of the expression, $\text{sgn}_n$ is introduced so that when the $n$-th effect is negative, it should be "-." In other words, the equilateral triangle and square are considered as a circle with numerous petal shaped disturbances.

The left side of (25) represents the disturbed part of the boundary $r_{shape}$ on a unit circle ($r(\theta) = 0.5$), which can be transformed into the summation of a series of sinusoidal functions. The negative sign to the right side of (25) is set to be consistent with the shape function of (1). For triangular and square shapes, the Fourier transform expressions are presented in the Appendix. By regarding the cross-sectional shape as the summation of a unit circle and a series of petal shapes, it follows from (23) and (24) that the ratio of static flow resistivity of a given shape to that of the unit circle is

$$k_{f\_shape}(s) = 1 + \sum_{n=1}^{\infty} \text{sgn}_n \cdot \left[ k_f(\varepsilon_n, n) - 1 \right]. \qquad (26)$$

Note that in each item of the series, the effect is subtracted by that of the unit circle, i.e., $k_f(\varepsilon_n, n) - 1$. Inserting Fourier transforms of triangle and square, i.e., Eqs. (A2) and (A4), into Eq. (26), we can obtain their relative static flow resistivities.
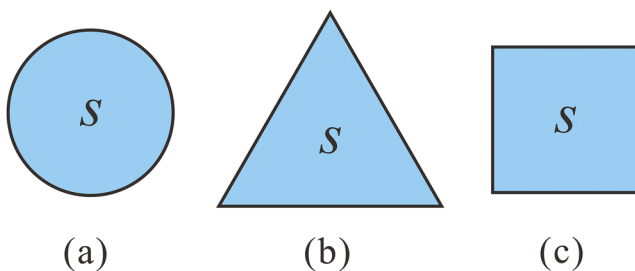


FIG. 2. (a) Circular, (b) equilateral triangular, and (c) square cross sections with identical area S.

## III. RESULTS AND DISCUSSION

### A. Validation against numerical simulation results

Numerical simulations with Computational Fluid Dynamics (CFD) software FLUENT are carried out on petal shaped pipes. Figure 3 displays the simulation settings. The left surface is set as the velocity inlet, and the right surface is set as the outflow. The boundary between the velocity inlet and outflow is set as the wall, and the fluid region inside is set as FLUID. Quadrilateral mesh is selected to sweep the whole region, and the maximum size of the grid is sufficiently small to ensure convergence of numerical simulation results: generally, if the grid number is more than 100 000, it can meet the requirement of mesh independence. In accordance with the assumption of small Reynolds numbers, the fluid velocity is set as 0.001 m/s. The CFD results are used to validate the theoretical model predictions, as illustrated below.

### B. Velocity distribution

With the wave number fixed at 6 (i.e., $n = 6$), Fig. 4(a) displays the remarkable influence of relative roughness on the velocity field in a petal shaped pipe ($D = 1$ mm), as obtained separately from the present theoretical model and CFD simulation. Corresponding results for the case of fixed relative roughness ($\varepsilon = 0.1$) but varying wave number are presented in Fig. 4(b). Overall, the comparison between model prediction and numerical simulation is reasonably well. As the same conclusion holds for other combinations of the wave number and relative roughness, the results are not presented here for brevity.

The results of Fig. 4 show that, due to the no-slip boundary condition, the velocity at the boundary is zero and the closer to the pipe center, the greater the fluid velocity. To examine clearly the difference in velocity fields between the theoretical and numerical results, line-scatter figures are presented in Fig. 5. It shows that the theoretical predictions agree well with the numerical simulations in a whole. The predicted velocities at the center are greater than the corresponding numerical ones, especially when the relative roughness or wave number is small. This occurs because when solving the perturbation equation, the logistic function form is assumed to characterize the two asymptotic limits so that the two parameters E and F in Eq. (12) can be determined. It
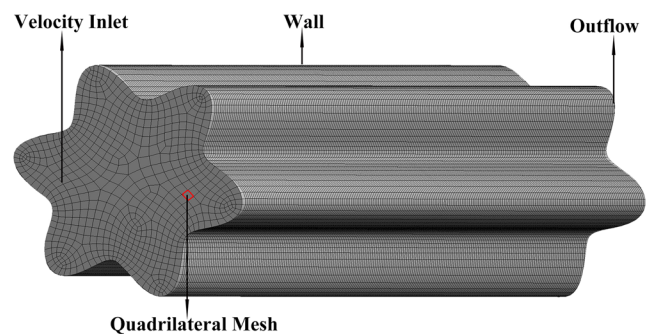


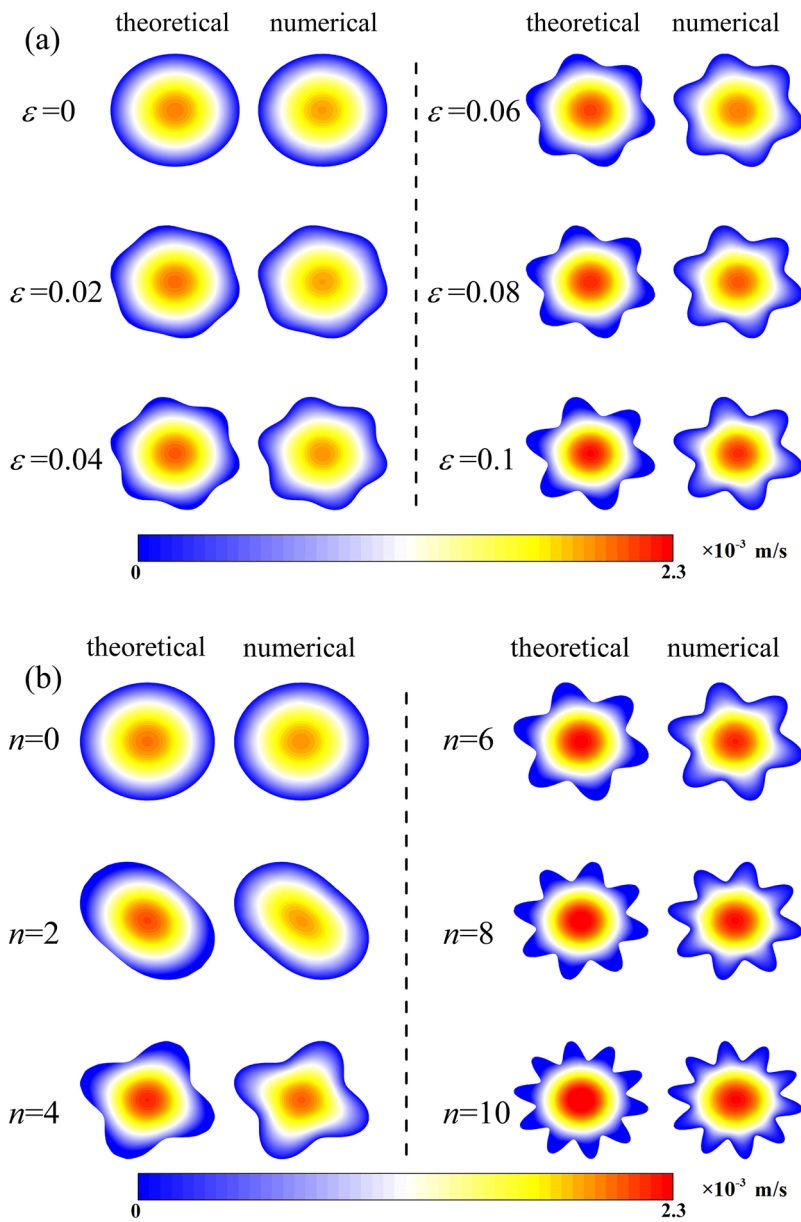FIG. 3. Sketch of numerical simulations with FLUENT.

FIG. 4. Comparison between theoretically predicted and numerically simulated velocity fields as contour maps in petal shaped pipes: (a) $n = 6$ and (b) $\varepsilon = 0.1$.
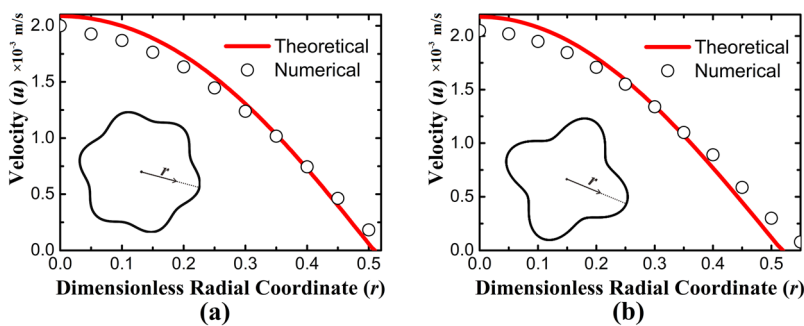


FIG. 5. Comparison between theoretically predicted and numerically simulated velocity fields as line-scatter figures in petal shaped pipes: (a) $n = 6$, $\varepsilon = 0.06$ and (b) $n = 4$, $\varepsilon = 0.1$.
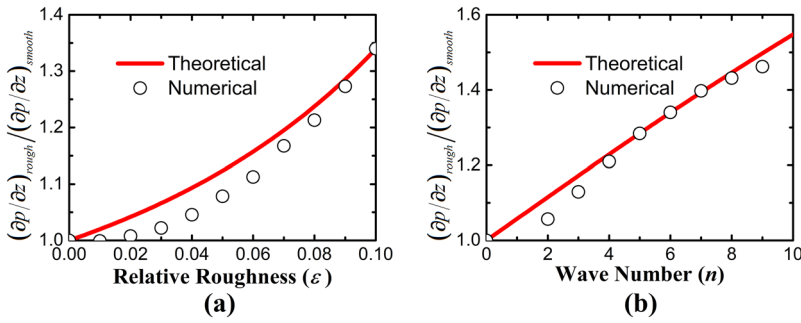
FIG. 6. Influence of surface roughness on the pressure gradient in a petal shaped pipe: (a) $n = 6$ and (b) $\varepsilon = 0.1$.

should, however, be pointed that, as an approximate approach, this inevitably involves certain errors, thus causing the discrepancy between the analytically predicted and numerically calculated velocities.

As for the influence of petal shapes, as shown in Fig. 4, upon changing the boundary morphology from a circle into a petal shape, the velocity contours also exhibit a petal-like shape, especially when the relative roughness or wave number is increased. From Eq. (21), we find that the disturbance of the pipe boundary affects the velocity field in two ways. One is reflected by the term containing $\theta$, representing the change in the shape of the velocity contour. The other is reflected by the term without $\theta$, representing the global offset of the velocity field. It should be pointed out that, in the presence of surface roughness, the fluid in the protruding portions of the petal shaped pipe is trapped (i.e., $u = 0$) due to the fluid viscosity and no-slip boundary condition. This feature is well captured by the proposed theoretical model.

## C. Pressure gradient

Boundary disturbance also affects significantly the pressure gradient in petal shaped pipes. As described in Eq. (2), the pressure gradient is the second derivative of the fluid velocity. Substituting the velocity field [Eq. (21)] into the Stokes equation, i.e., Eq. (2), we find that the second derivative of the period term containing $\theta$ in the velocity expression is zero. This implies that there is no period term in the pressure gradient. It is thus interesting to observe that while the velocity field inside a petal shaped pipe exhibits periodic disturbance, the pressure gradient is constant over a specified cross section. The latter actually ensures that the fluid field is symmetrical.

The theoretical predictions and numerical results of the pressure gradient inside a petal shaped pipe (normalized by that inside a smooth circular pipe) are compared in Fig. 6 for selected values of wave number and relative roughness. Again, reasonably good agreement is achieved. Relative to a circular pipe (either $\varepsilon = 0$ or $n = 0$), the pressure gradient in a petal shaped pipe is much greater. As the relative roughness and/or wave number is increased, the perimeter of the pipe cross section becomes longer, which implies more contact area between the fluid and the solid wall. The wall imposes a drag force to the flowing fluid due to its viscosity, increasing as the surface roughness of the pipe is increased. In fully developed flow, this drag force is balanced with the pressure difference.

## D. Static flow resistivity

The flow resistance depends largely on the parameters characterizing the rough structure, as shown in Fig. 7. The influence of the relative roughness and wave number on relative static flow resistivity is quantified theoretically and numerically. Theoretical expressions of the static flow resistivity for petal shaped pipes are given in Eqs. (23) and (24). Table I presents further explicit expressions of static flow resistivity by taking the Taylor expansion and retaining terms up to $\varepsilon^2$ (which ensures the accuracy of calculation). The agreement between the theory and numerical simulation is good. As the relative roughness increases, the relative static flow resistivity rises, increasing more sharply [Fig. 7(a)]. By contrast, the results of Fig. 7(b) show that as the wavenumber increases, the numerically calculated relative static flow resistivity first rises and then tends to an upper limit. In comparison, the theoretical model predictions deviate from the
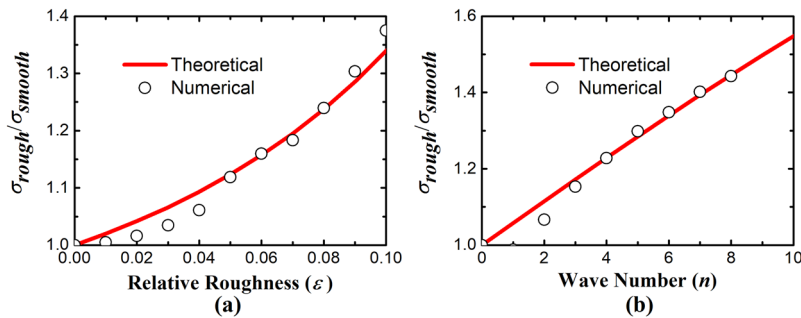


FIG. 7. Comparison of static flow resistivity between theoretical predictions and numerical calculations: (a) $n = 6$ and (b) $\varepsilon = 0.1$.

**TABLE I**. Theoretically predicted static flow resistivity ($\sigma$) of petal shaped pipes with varying wave numbers and relative roughness.

| Wave number $n$ | Shape | $\sigma$ |
|---|---|---|
| $n = 1$ | | $\left(1 + 0.32\varepsilon + 1.6\varepsilon^2\right)\frac{8\mu}{a^2}$ |
| $n = 2$ | | $\left(1 + 0.64\varepsilon + 3.2\varepsilon^2\right)\frac{8\mu}{a^2}$ |
| $n = 3$ | | $\left(1 + 0.96\varepsilon + 4.8\varepsilon^2\right)\frac{8\mu}{a^2}$ |
| $n = 4$ | | $\left(1 + 1.28\varepsilon + 6.4\varepsilon^2\right)\frac{8\mu}{a^2}$ |
| $n = 5$ | | $\left(1 + 1.6\varepsilon + 8\varepsilon^2\right)\frac{8\mu}{a^2}$ |
| $\dots$ | $\dots$ | $\dots$ |
| $n = \infty$ | $\dots$ | $\left(1 + 8\varepsilon + 40\varepsilon^2\right)\frac{8\mu}{a^2}$ |

**TABLE II**. Static flow resistivity ($\sigma$) for circular, triangular, and square pipes: comparison between the present model and the existing study.

| Cross-sectional morphology | $\sigma$ (present study) | $\sigma$ (Ref. 27) |
|---|---|---|
| circle | $\frac{8\mu}{a^2}$ | $\frac{8\mu}{a^2}$ |
| triangle | $\frac{76.95\mu}{a^2}$ | $\frac{80\mu}{a^2}$ |
| square | $\frac{28.46\mu}{a^2}$ | $\frac{28.4\mu}{a^2}$ |

numerical results when the wave number is small. When $n$ is small (e.g., $n = 1, 2$), the pipe cross section is yet to develop into a periodic petal-like structure, reducing thus the effectiveness of the calculation process. Furthermore, as different morphologies of the cross section require different grids for simulation, the accuracy of numerical results varies among the morphologies considered.
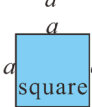
From Table I, it is seen that as the wave number increases, the static flow resistivity also increases, which is consistent with Fig. 7(b); when the wave number becomes infinitely large, the static flow resistivity approaches asymptotically its upper limit. Increasing the wave number enables more fluid to be trapped due to its viscosity and the no-slip condition, and hence it becomes harder for the fluid to pass through. The results of Table I also reveal that when the wave number is small, the static flow resistivity is approximately linearly proportional to the wave number, providing thus a quick way to estimate the effect of the wave number on static flow resistivity.

### E. Triangular and square pipes

In Secs. III B–III D, the flow field, pressure gradient, and static flow resistivity of petal shaped pipes have been obtained using the modified perturbation method. It is interesting that the same method can be combined with Fourier transform to deal with triangular and square pipes, as demonstrated in Sec. II C and the Appendix.

Table II compares the static flow resistivity predicted by the present model with that obtained by Bruus *et al.*[27] for circular, triangular, and square pipes. Excellent agreement is achieved, validating again the modified perturbation method proposed in the present study.

## IV. CONCLUSION

A theoretical model has been established to estimate the fully developed flow at a small Reynolds number (Stokes flow) inside petal shaped pipes by regarding the pipe wall as a circular boundary with sinusoidal perturbation (or, equivalently, surface roughness). The effects of the relative roughness and wave number of the petal shaped pipe wall are quantified using the modified perturbation method. Approximate solutions of the velocity field, pressure gradient, and static flow resistivity are obtained, which are validated by results obtained from direct numerical simulations. The main findings are summarized as follows:

(1) The presence of surface roughness leads to periodic fluctuation and global offset of velocity distribution.
(2) Increasing the relative roughness or wave number of the pipe wall enlarges both the pressure gradient and static flow resistivity.
(3) For relatively small wave numbers of roughness, the static flow resistivity is linearly proportional to the wave number.
(4) With the triangle or square taken as the summation of a series of sinusoidal perturbations and a unit circle, the flow resistivity inside triangular and square pipes can be obtained via Fourier transform.

## APPENDIX: FOURIER TRANSFORM EXPRESSIONS FOR THE BOUNDARY CURVE FUNCTIONS OF TRIANGULAR AND SQUARE SHAPES

With reference to Fig. 2, because the equilateral triangle and square are assumed to have an identical cross-sectional

area as the unit circle (with radius $r = 0.5$), the side length of the triangle is $\sqrt{\pi/\sqrt{3}}$, while that of the square is $\sqrt{\pi}/2$. Their Fourier transforms are presented below so that the flow field is equivalent to that obtained from the summation of a series of petal shaped pipes.

The boundary curve function of the equilateral triangle is expressed using a piecewise function as

$$r_{triangle}(\theta) = \begin{cases} \dfrac{\sqrt{\pi/\sqrt{3}}/2\sqrt{3}}{\cos(\theta - \pi/6)}, & -\dfrac{\pi}{6} < \theta < \dfrac{\pi}{2} \\[2mm] \dfrac{\sqrt{\pi/\sqrt{3}}/2\sqrt{3}}{\cos(\theta - 5\pi/6)}, & \dfrac{\pi}{2} < \theta < \dfrac{7\pi}{6} \\[2mm] \dfrac{\sqrt{\pi/\sqrt{3}}/2\sqrt{3}}{\cos(\theta - 3\pi/2)}, & \dfrac{7\pi}{6} < \theta < \dfrac{11\pi}{6} \end{cases} \quad (A1)$$

Regarding the boundary curve as the summation of a series of petal shapes with increasing wave numbers, we can obtain Fourier transform of the triangle. Here, to assure the accuracy of calculation, we obtain Fourier transform by retaining items up to 9 as

$$\begin{aligned} r_{triangle}(\theta) - 0.5 = &-0.010\,86 \sin(\theta) - 0.132\,19 \sin(3\theta) \\ &+ 0.026\,34 \sin(5\theta) - 0.038\,15 \sin(7\theta) \\ &+ 0.009\,28 \sin(9\theta) + \ldots. \end{aligned} \quad (A2)$$

For the case of a square pipe, the boundary curve function is

$$r_{square}(\theta) = \begin{cases} \dfrac{\sqrt{\pi}/2/2}{\cos(\theta)}, & -\dfrac{\pi}{4} < \theta < \dfrac{\pi}{4} \\[2mm] \dfrac{\sqrt{\pi}/2/2}{\cos(\theta - \pi/2)}, & \dfrac{\pi}{4} < \theta < \dfrac{3\pi}{4} \\[2mm] \dfrac{\sqrt{\pi}/2/2}{\cos(\theta - \pi)}, & \dfrac{3\pi}{4} < \theta < \dfrac{5\pi}{4} \\[2mm] \dfrac{\sqrt{\pi}/2/2}{\cos(\theta - 3\pi/2)}, & \dfrac{5\pi}{4} < \theta < \dfrac{7\pi}{4} \end{cases} \quad (A3)$$

Similarly, to assure the accuracy of calculation, we obtain Fourier transform by retaining items up to 9 as

$$\begin{aligned} r_{square}(\theta) - 0.5 = &-0.00246 \sin(\theta) + 0.03363 \sin(3\theta) \\ &- 0.05339 \sin(5\theta) - 0.03185 \sin(7\theta) \\ &+ 0.0032 \sin(9\theta) + \ldots. \end{aligned} \quad (A4)$$

## REFERENCES

[1] K. Huang, J. W. Wan, C. X. Chen, Y. Q. Li, D. F. Mao, and M. Y. Zhang, "Experimental investigation on friction factor in pipes with large roughness," Exp. Therm. Fluid Sci. **50**, 147–153 (2013).

[2] F. Dierich and P. A. Nikrityuk, "A numerical study of the impact of surface roughness on heat and fluid flow past a cylindrical particle," Int. J. Therm. Sci. **65**, 92–103 (2013).

[3] R. Von Mises, "Elemente der technischen hydromechanik," Monatsh. Math. Phys. **26**, A27–A28 (1915).

[4] C. F. Colebrook and C. M. White, "Experiments with fluid friction in roughened pipes," Proc. R. Soc. London, Ser. A **161**, 367–381 (1937).

[5] C. F. Colebrook, T. Blench, H. Chatley, E. Essex, J. Finniecome, G. Lacey, J. Williamson, and G. Macdonald, "Turbulent flow in pipes with particular reference to the transition region between smooth and rough pipe laws," J. Inst. Civ. Eng. **12**, 393–422 (1939).

[6] J. Nikuradse, "Laws of flow in rough pipes," Technical Report Archive and Image Library, 1950.

[7] L. F. Moody, "Friction factors for pipe flow," Trans. ASME **66**, 671–684 (1944).

[8] C. Pozrikidis, "The flow of a liquid film along a periodic wall," J. Fluid Mech. **188**, 275–300 (2006).

[9] W. Qu, G. M. Mala, and D. Li, "Pressure-driven water flows in trapezoidal silicon microchannels," Int. J. Heat Mass Transfer **43**, 353–364 (2000).

[10] D. J. Schmitt and S. G. Kandlikar, "Effects of repeating microstructures on pressure drop in rectangular minichannels," in *Third International Conference on Microchannels and Minichannels* (ASME, Toronto, Ontario, Canada, 2005), pp. 281–289.

[11] V. V. Dharaiya and S. G. Kandlikar, "A numerical study on the effects of 2d structured sinusoidal elements on fluid flow and heat transfer at microscale," Int. J. Heat Mass Transfer **57**, 190–201 (2013).

[12] S. Siddiqa, M. A. Hossain, and R. S. R. Gorla, "Natural convection flow of viscous fluid over triangular wavy horizontal surface," Comput. Fluids **106**, 130–134 (2015).

[13] S. G. Kandlikar, D. Schmitt, A. L. Carrano, and J. B. Taylor, "Characterization of surface roughness effects on pressure drop in single-phase flow in minichannels," Phys. Fluids **17**, 100606 (2005).

[14] J. Zou and X. F. Peng, "Effects of roughness on liquid flow behavior in ducts," in *ASME 2006 Joint U.S.-European Fluids Engineering Summer Meeting Collocated with the International Conference on Nuclear Engineering* (ASME, USA, 2006), pp. 49–56.

[15] R. N. Wagner and S. G. Kandlikar, "Effects of structured roughness on fluid flow at the microscale level," Heat Transfer Eng. **33**, 483–493 (2012).

[16] M. R. Stinson and Y. Champoux, "Propagation of sound and the assignment of shape factors in model porous materials having simple pore geometries," J. Acoust. Soc. Am. **91**, 685–695 (1992).

[17] N. A. Mortensen, F. Okkels, and H. Bruus, "Reexamination of Hagen-Poiseuille flow: Shape dependence of the hydraulic resistance in microchannels," Phys. Rev. E **71**, 057301 (2005).

[18] K. Attenborough and O. Buser, "On the application of rigid-porous models to impedance data for snow," J. Sound Vib. **124**, 315–327 (1988).

[19] W. E. Wiesel, *Modern Astrodynamics* (Createspace, USA, 2010).

[20] M. Van Dyke, *Perturbation Methods in Fluid Mechanics* (Academic press, New York, USA, 1964).

[21] J. J. Chattot and M. M. Hafez, *Inviscid, Compressible Flow Past Thin Airfoils* (Springer, Holland, The Netherlands, 2015).

[22] S. Song, X. Yang, F. Xin, and T. J. Lu, "Modeling of surface roughness effects on Stokes flow in circular pipes," Phys. Fluids **30**, 023604 (2018).

[23] K. H. Chu, "Stokes slip flow between corrugated walls," Z. Angew. Math. Mech. **47**, 591–599 (1996).

[24] C. Y. Wang, "On Stokes slip flow through a transversely wavy channel," Mech. Res. Commun. **38**, 249–254 (2011).

[25] D. Hosmer and S. Lemeshow, *Applied Logistic Regression*, 2nd ed. (Wiley-Interscience, USA, 2000).

[26] ASTM 522-3: Standard Test Method for Airflow Resistance of Acoustical Materials, American Society for Testing and Materials, West Conshohocken, PA, 2009.

[27] H. Bruus, "Acoustofluidics 1: Governing equations in microfluidics," Lab Chip **11**, 3742–3751 (2011).